

University of Groningen

X-ray photoabsorption-induced processes within protonated rifamycin sodium salts in the gas phase

Abdelmouleh, Marwa; Espinosa Rodriguez, Andrea; Leroux, Juliette; Christodoulou, Pinelopi; Bernay, Benoît; Schlathölter, Thomas; Pouilly, Jean-Christophe

Published in:
European Physical Journal D

DOI:
[10.1140/epjd/s10053-021-00092-w](https://doi.org/10.1140/epjd/s10053-021-00092-w)

IMPORTANT NOTE: You are advised to consult the publisher's version (publisher's PDF) if you wish to cite from it. Please check the document version below.

Document Version
Publisher's PDF, also known as Version of record

Publication date:
2021

[Link to publication in University of Groningen/UMCG research database](#)

Citation for published version (APA):

Abdelmouleh, M., Espinosa Rodriguez, A., Leroux, J., Christodoulou, P., Bernay, B., Schlathölter, T., & Pouilly, J-C. (2021). X-ray photoabsorption-induced processes within protonated rifamycin sodium salts in the gas phase. *European Physical Journal D*, 75(3), [74]. <https://doi.org/10.1140/epjd/s10053-021-00092-w>

Copyright

Other than for strictly personal use, it is not permitted to download or to forward/distribute the text or part of it without the consent of the author(s) and/or copyright holder(s), unless the work is under an open content license (like Creative Commons).

The publication may also be distributed here under the terms of Article 25fa of the Dutch Copyright Act, indicated by the "Taverne" license. More information can be found on the University of Groningen website: <https://www.rug.nl/library/open-access/self-archiving-pure/taverne-amendment>.


Take-down policy

If you believe that this document breaches copyright please contact us providing details, and we will remove access to the work immediately and investigate your claim.

Downloaded from the University of Groningen/UMCG research database (Pure): <http://www.rug.nl/research/portal>. For technical reasons the number of authors shown on this cover page is limited to 10 maximum.



X-ray photoabsorption-induced processes within protonated rifamycin sodium salts in the gas phase

Marwa Abdelmouleh¹, Andrea Espinosa Rodriguez^{1,2}, Juliette Leroux¹, Pinelopi Christodoulou^{1,3}, Benoît Bernay⁴, Thomas Schlathöler⁵, and Jean-Christophe Pouilly^{1,a} 

¹ CIMAP UMR 6252 (CEA/CNRS/ENSICAEN/Université de Caen Normandie), Boulevard Becquerel, 14070 Caen Cedex 5, France

² Grupo de Física Nuclear, Dpto. de Estructura de la Materia, Física Térmica y Electrónica, Facultad de CC Físicas, GFN-UCM, Avda. Complutense, s/n, 28040 Madrid, Spain

³ Faculty of Biomedical Engineering, Czech Technical University in Prague, nám. Sítná 3105, 272 01 Kladno 2, Prague, Czech Republic

⁴ Université de Caen Normandie, Plateforme PROTEOGEN, SF 4206 ICORE, Esplanade de la paix, 14032 Caen, France

⁵ Zernike Institute for Advanced Materials, University of Groningen, Nijenborgh 4, 9747AG Groningen, The Netherlands

Received 7 December 2020 / Accepted 17 February 2021

© The Author(s), under exclusive licence to EDP Sciences, SIF and Springer-Verlag GmbH Germany, part of Springer Nature 2021

Abstract. Up to now, the response of antibiotics upon ionizing radiation has been very scarcely reported. Here, we present the results of X-ray photoabsorption experiments on isolated rifamycin, a broad-range antibiotic against Gram-positive and Gram-negative bacteria. A mass spectrometer has been coupled to a synchrotron beamline to analyze cationic products of photoabsorption on protonated rifamycin dimer and monomer sodium salts. Absorption of a single photon in the 100–300eV energy range leads to ionization of the molecular system, followed by vibrational energy deposition and subsequent inter- and/or intramolecular fragmentation. Interestingly, we observe a proton transfer from sodiated rifamycin to rifamycin, a widely observed process in ionized molecular systems in the gas phase. Moreover, we show that another charge-transfer process occurs in both dimer and monomer: intramolecular sodium transfer, which has not been reported yet, to the best of our knowledge.

1 Introduction

Advances in mass spectrometry and soft ionization techniques have over the last decades led to an enormous increase of interest in the properties of isolated molecular systems. In particular, biologically relevant systems have attracted much interest and applications can now be found in very diverse fields, most prominently in the so-called multiomics (proteomics, metabolomics and lipidomics...), but also in the tracing of cancer cell metabolites [1] or the characterization of ligand–receptor noncovalent complexes [2]. Mass spectrometry also allows analyzing the product ions from interactions between ionizing radiation and biomolecular systems in the gas phase with the aim of shedding light on the radiation-induced physical and chemical processes on the molecular level. Controlling these processes is crucial for optimizing the efficiency of new techniques aiming at the degradation of antibiotics in water: the contemporary extensive use of antibiotics combined with their poor natural degradation properties has led to a persistent contamination of our aqueous environment [3]. We have

recently studied the irradiation of vancomycin, a last-resort antibiotic against Gram-positive bacteria, by means of VUV as well as soft X-ray photons in the gas phase [4,5]. Extensive fragmentation following ionization and vibrational energy deposition was found to occur. In this work, we investigate the response of isolated rifamycin SV upon soft X-ray irradiation. This molecule belongs to a family of antibiotics that are naturally produced by *Amycolatopsis mediterranei* and has a broad spectrum of activity against Gram-positive and Gram-negative bacteria. One of the most severe diseases that is efficiently treated with rifamycins is HIV-related tuberculosis. The mechanism of action involves inhibiting in a very selective manner the bacterial DNA-dependent RNA polymerase via noncovalent binding [6]. Rifamycin SV (abbreviated rifamycin in the following) was the first drug of the rifamycin family to be clinically used. Its photodegradation upon visible light irradiation has been investigated in solution, disentangling direct and indirect effects and demonstrating that one of the mechanisms of degradation is due to direct absorption of light [7]. However, the authors did not identify the degradation products. Here, we show mass spectra of the cationic products formed after X-ray photoabsorption in isolated rifamycin, as well as the evolu-

^a e-mail: pouilly@ganil.fr (corresponding author)

tion of their abundance with respect to photon energy, to shed light on the direct effects of irradiation.

2 Experimental methods

Rifamycin SV was purchased from Sigma-Aldrich as a sodium salt in powder and used without further purification. Solutions were prepared in 50:50 (volume ratio) water/methanol at 50 μM concentration with 1 % of formic acid to protonate the molecules.

Collision-induced dissociation (CID) experiments were performed using a commercial apparatus coupling trapped ion mobility spectrometry and time-of-flight mass spectrometry (TIMS-TOF Pro, Bruker Daltonics) [8]. Protonated molecules were brought to the gas phase by means of a modified nano-electrospray ionization source (CaptiveSpray, Bruker Daltonics). The syringe flow rate was 300 $\mu\text{L}/\text{h}$, the voltage difference between the needle and the capillary was 4500 V, and the drying gas flow rate and temperature were 3.0 L/mn and 200 $^{\circ}\text{C}$, respectively. The capillary was kept at room temperature. Mainly sodiated rifamycin was produced by the source. After the ions exited the capillary, they were focused by a funnel and injected into the TIMS cell where air flowed at a pressure of 2–3 mbar and at room temperature. The ions were trapped for 309.6ms along the cell's longitudinal axis at a position that depends on their charge and their collision cross section with air. Indeed, the ions are trapped when the magnitude of the air dragging force equals that of the counteracting electric force. After extraction, the ions were focused by two funnels and guided through a hexapole. Then, the ions of interest were mass-overcharge-selected by a quadrupole (isolation width 1 Da) and injected into a collision cell filled with nitrogen. The collision energy was scanned between 10 and 65 eV. The product ions were analyzed by a two-stage reflectron and finally detected by microchannel plates. The system was calibrated each week, and mass precision was better than 1 ppm. Mass spectra were acquired in positive mode in the m/z 20–1000 range. In the experiments described here, the mass spectrometer was operated in MS/MS mode.

A home-built tandem mass spectrometer, described in detail elsewhere, [9] has been used to record mass spectra of the cationic photo-products from the interaction between molecular systems and synchrotron radiation. Briefly, protonated molecular systems are produced with an electrospray ionization (ESI) source and transported into the vacuum chamber through a capillary, which is heated to help desolvation of the molecular ions, because of the absence of drying gas. Here again, mainly sodiated rifamycin was produced by the source. All ions created by the source are focused into an ion funnel and guided into an octopole RF device. Then, the molecular ions of interest are mass-overcharge-selected with a quadrupole mass filter and subsequently accumulated in a 3D radiofrequency ion Paul

trap. Trapping is facilitated by collisions with a helium buffer gas duration injected into the ion trap during 50–100 ms. After a 100 ms delay to allow pumping down the helium, trapped molecular ions are then irradiated by X-ray photons at the U49-2 PGM-1 beamline of the BESSY II synchrotron (Helmholtz-Zentrum Berlin). Photon beam exposure of the trap content, typically during 100 to 1000 ms, is controlled with a mechanical shutter in order to guarantee that more than 90 % of the product cations result from the absorption of a single photon. To do so, the irradiation time is tuned to induce a depletion of the precursor ion below 10 %. Since the absorption of multiple photons is a sequential process at these fluxes (10^{12-13}s^{-1}), the absorption events are independent; thus, a probability p for absorbing one photon gives the probability p^2 for two photons. Neglecting the absorption of more than two photons, we obtain $p^2 + p < 0.1$ and thus $p < 0.09$. Precursor ions and cationic fragments are then extracted from the trap by applying a high voltage pulse to the hyperbolic end caps, analyzed by a time-of-flight reflectron mass spectrometer, and detected by a microchannel plate detector with a post-acceleration voltage of -5kV. The signal is recorded by a 1 GHz digitizer. Mass spectra of the nonirradiated trap content (beam-off) and irradiated residual gas are recorded as well, the latter allowing to identify background peaks due to photoionization of residual gas molecules. Then, the beam-on mass spectrum is subtracted from the beam-off one, and the resulting spectrum shows the precursor ion depletion with a negative intensity. Assuming that absorption of one photon leads to ionization and/or fragmentation of the precursor ion, this depletion (area under the peak) is proportional to the total photo-absorption yield. All relative yields have been obtained by calculating the area under each peak, normalizing by the precursor ion depletion, by the total yield of all cationic species formed by photoabsorption and by detection efficiency [10].

3 Results and discussion

3.1 Sodiated rifamycin is a protonated molecular salt

First, we will provide evidence that isolated sodiated rifamycin is a protonated molecular salt, which means that the sodium ion is bound to a deprotonated group, forming an ionic bond that is much stronger than other noncovalent bonds between sodium and neutral molecules. We have investigated the lowest-energy fragmentation channels of sodiated and protonated rifamycin by means of CID on nitrogen. The experiments have been performed with a commercial mass spectrometer that includes an ESI source to bring rifamycin in the gas phase (see Sect. 2 for details). Figure 1 shows the CID spectra of protonated rifamycin (m/z 698) at collision energies of 10, 30 and 50 eV. At 10 eV, the most intense peaks are observed at m/z 666

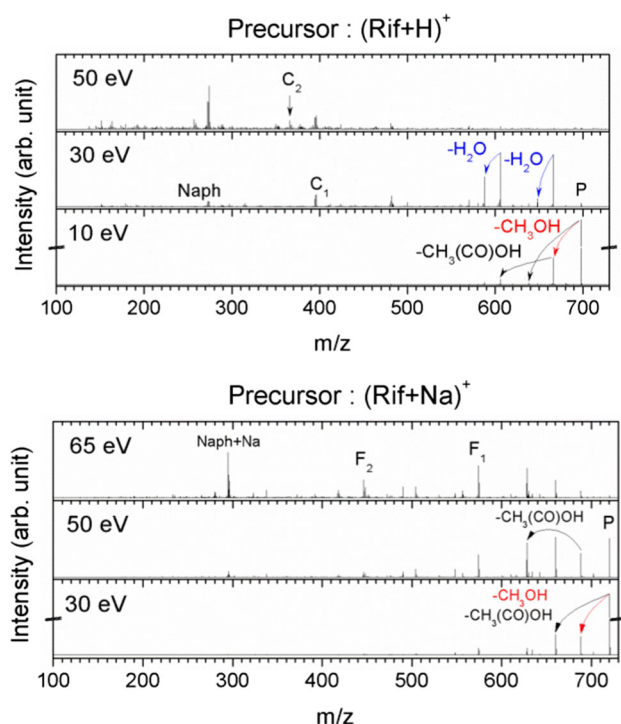


Fig. 1 Mass spectra of protonated rifamycin (top, m/z 698) and sodiated rifamycin (bottom, m/z 720) after CID at different collision energies. The position of precursor ions is noted P, loss of neutral molecules is indicated by arrows, and the main fragments involving cleavage of two bonds are also noted

and 606: we assign them to fragment ions formed after loss of CH_4O ($698 - 666 = 32$ Da) and successive loss of $\text{C}_2\text{H}_4\text{O}_2$ ($666 - 606 = 60$ Da). Loss of small neutral molecules from protonated species is a well-known process, observed for instance in protonated peptides and explained by the mobile proton model [11]. Loss of CH_3OH (methanol) has been widely reported after CID of protonated molecules, and the proposed mechanism implies a proton transfer to the oxygen of a CH_3O group [12–18]. Since rifamycin contains such a group (*cf.* Fig. 2), the same mechanism can be inferred here. Moreover, Komaromi et al. calculated potential energy barriers of 1–2 eV for proton transfer followed by methanol loss in N-acetyl OMe proline, supporting the presence of methanol loss in low-energy CID spectra [15]. Rifamycin also contains a $\text{CH}_3(\text{CO})\text{O}$ group; therefore, one can expect that loss of $\text{CH}_3(\text{CO})\text{OH}$ (acetic acid) can be explained by the same proton transfer mechanism in the fragment ion of m/z 666.

At higher collision energy (30 eV), additional peaks appear (*cf.* Fig. 1). The ones at m/z 648 and 588 correspond to loss of H_2O (18 Da) from the fragment ions of m/z 666 and 606, respectively, probably due to proton transfer to an OH group, like the neutral losses seen at a collision energy of 10 eV. m/z 273 corresponds to the naphthofuran group (see Fig. 2) noted Naph, which is formed by cleavage of two bonds. This fragment has been observed previously in CID of depro-

tonated rifamycin [19]. If the charge remained on the other part of rifamycin, it would form a fragment ion of m/z $698 - 273 = 425$. We observe many peaks in the m/z 400–450 region of the spectrum: they are separated by m/z 1, which is usually attributed to H scrambling between fragments, due to activation of the molecule by collisions with the gas. The abundance of the peaks around m/z 425 is low, but the peaks at m/z 394, 395 and 396 are more intense: we assign them to loss of CH_3OH from protonated rifamycin accompanied by H scrambling, cleavage of the two bonds mentioned above and formation of a fragment noted C_1 . At even higher collision energy (50 eV, see Fig. 1), peaks of high m/z disappear and some appear in the lower m/z region, notably at m/z 366, the most intense ones being Naph and C_1 . We assign the peak at m/z 366 to a fragment called C_2 , formed by loss of $\text{CH}_3(\text{CO})\text{OH}$ followed by loss of the Naph fragment.

The mass spectra obtained by CID of sodiated rifamycin (m/z 720) are also shown in Fig. 1: at a collision energy of 30 eV, the same low-energy processes as those for protonated rifamycin are observed, namely loss of neutral methanol and acetic acid. The similarity between the two forms of rifamycin (protonated and sodiated) also remains when collision energy rises up to 65 eV, since the naphthofuran fragment appears and becomes dominant. Interestingly, for sodiated rifamycin this fragment is observed at m/z 295, which corresponds to the *sodiated* naphthofuran fragment noted Naph+Na (note that Na substitutes one H). This is consistent with the structure of sodiated rifamycin provided by the PubChem database, where sodium is bound to an oxygen of the naphthofuran group (PubChem ID 23702994 [20]). Additional fragments at m/z 574 (noted F_1) and 446 (noted F_2) are also observed: they also include the sodiated naphthofuran group, and we propose structures for them in Fig. 2. Note that the putative fragment ion complementary to Naph and containing sodium would be found at m/z 446.228, whereas F_2 is predicted at m/z 446.122, which is much closer to the detected m/z 446.120. These observations support the fact that in both protonated and sodiated rifamycin, the same processes are triggered by collisions on nitrogen, probably proton transfer followed by bond cleavage. This is in line with sodiated rifamycin being a molecular salt in the gas phase, with the sodium ion bound to a deprotonated oxygen, forming a strong ionic bond and leaving the charge to a proton. The same behavior has been observed for gas-phase sodiated lasalocid acid (another antibiotic) [21] as well as for sodiated lysoglycerophospholipids [22] formed by ESI.

3.2 X-ray photoabsorption of the sodiated rifamycin dimer

We have irradiated the sodiated rifamycin dimer containing two rifamycin molecules and one sodium (m/z 1417) by soft X-rays at different photon energies in the 100–300 eV range, and the results are shown in Fig. 3. In the mass spectrum of cationic products

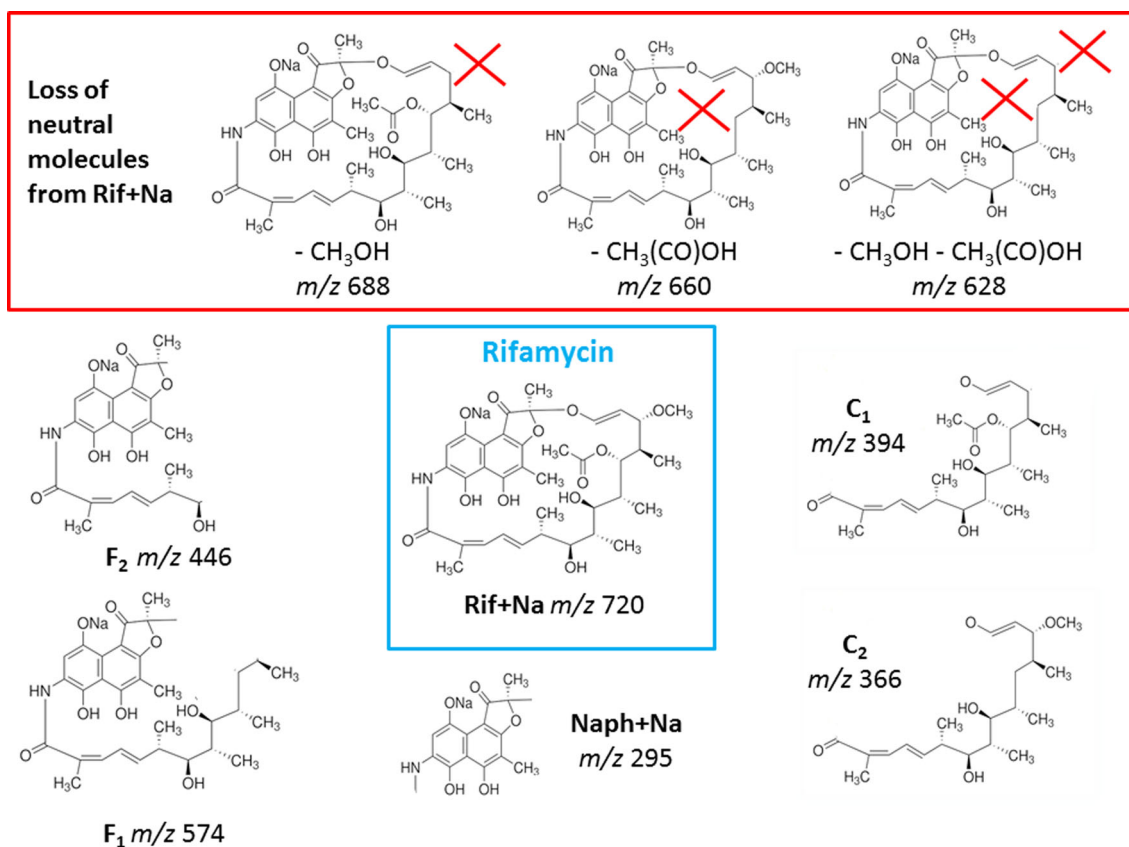


Fig. 2 Chemical structure of sodiated rifamycin [20] (noted Rif+Na ; PubChem ID 23702994) and proposed chemical structures for some of its fragments. Rifamycin is formed by substituting Na by H. The m/z values indicated for rifamycin and fragments due to loss of neutral molecules correspond to protonated species. Red crosses spot the sites of lost groups

formed after absorption of one 100 eV photon, we can observe the dominance of peaks assigned to rifamycin monomers, with and without sodium. An enlargement of this part of the spectrum is also shown in Fig. 3: the most intense peaks are due to the rifamycin radical cation at m/z 697 and sodiated rifamycin at m/z 720, which are complementary fragments of the precursor ion. Their formation can thus be explained by dissociation of the dimer after ionization. At 100 eV photon energy, only valence electrons of the precursor ion are ejected, since the 1s orbitals of lowest binding energy are the carbon ones around 290 eV [23]. At this energy, we have already observed extensive cleavage of noncovalent bonds within other molecular complexes [4, 24]. Interestingly, the peak at m/z 698 is too intense to be attributed only to the ¹³C isotope of the rifamycin radical cation (62% instead of 42% of the intensity at m/z 697): the difference is most probably due to protonated rifamycin, formed after proton or H transfer from sodiated rifamycin. The presence of a peak at m/z 719 (sodiated rifamycin - H) supports this hypothesis. Moreover, proton transfer has already been observed many times within gas-phase noncovalent complexes after ionization, even in the absence of H-bonds [5, 25–29]. It con-

firms that it is a general process in ionized molecular systems. Besides, it is consistent with the fact that the dimer is a protonated molecular salt, akin to the case of the sodiated rifamycin monomer (see Sect. 3.1).

The spectrum at the bottom of Fig. 3 also shows peaks at m/z 688, 660 and 666: they are assigned to loss of methanol and acetic acid from sodiated rifamycin and methanol from protonated rifamycin, respectively, after photoabsorption at 100 eV. The same channels have been observed after CID of these species (see Sect. 3.1); thus, we deduce that after photoabsorption, the dimer undergoes ionization and some of the photon energy is transferred into vibrational energy, causing dimer dissociation, and the rifamycin monomers subsequently lose neutral molecules. We have already observed these processes in several molecular systems in the gas phase, including noncovalent complexes, after single X-ray photoabsorption [4, 30]. Moreover, the other most intense peaks are assigned to the C₁ (m/z 394), Naph and Naph+Na fragments that we also already observed in CID experiments (see Fig. 1), confirming that fragmentation is mainly due to vibrational energy transfer to the system after photoabsorption. The most interesting peak is observed at m/z 416: it is extremely weak in rifamycin's CID spectra, and we

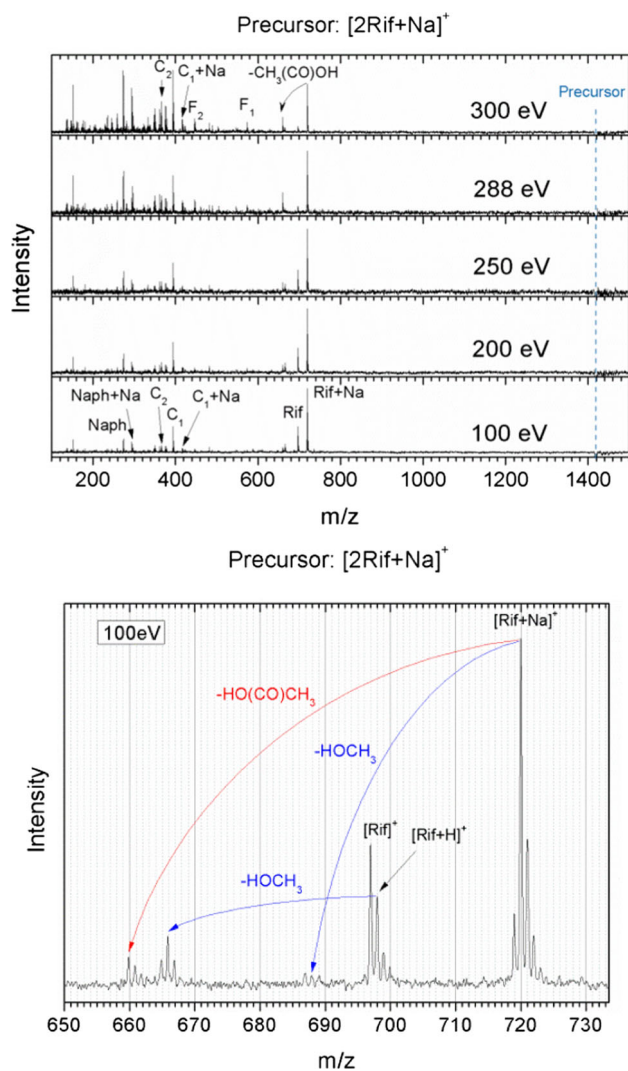


Fig. 3 Top: mass spectra of the sodiated rifamycin dimer after absorption of one soft X-ray photon; bottom: zoom of the mass spectrum at 100 eV photon energy in the m/z range where peaks assigned to rifamycin monomers as well as loss of neutral molecules are observed

assign it to C_1+Na .¹ Since Na is initially bound to the naphthofuran group in sodiated rifamycin, it indicates that sodium has been transferred to the other side of the molecule. Unlike proton transfer, gas-phase sodium transfer after ionization of molecular systems has not been reported yet, to the best of our knowledge. However, previous mass spectrometric studies involving sodium transfer do exist: for instance, Liang et al. [31] have observed sodium transfer from doubly sodiated glycerophosphocholine lipids to azobenzene radical anions in the gas phase, Blagojevic and Bohme

¹ As stated in the experimental section, to spot background peaks for each photon energy, we record a mass spectrum with the photon beam on and the ESI off, and another mass spectrum with the beam off and the ESI on. We did not find any signal at m/z 416 in any of these spectra.

[32] studied intermolecular sodium transfer to high proton affinity molecules, and Hoyau *et al.* [33] combined experiments and quantum-chemical calculations to provide accurate values of sodium affinities of organic molecules. From our results, we cannot know if sodium transfer within the sodiated rifamycin dimer is inter- or intramolecular. However, we can obtain more information by looking at the evolution of photoproducts as a function of photon energy.

When photon energy rises up to 300 eV, the mass spectrum of the sodiated rifamycin dimer changes quite strongly: the intensity of peaks assigned to fragments of monomers increase and largely dominate at 300 eV. At the latter energy, one can notice the presence of the F_1 and F_2 fragments (m/z 574 and 446) already observed in the high-energy CID spectra of sodiated rifamycin. The evolution of the sum of the abundances of rifamycin monomers and of the total yield of fragments after photoabsorption in the 100–300 eV range is depicted in Fig. 4: over the whole range, but more strongly from 288 eV, monomers' abundance decreases while that of fragments rises. This is attributed to an increase of the vibrational energy transferred to the molecular system for photons of at least 288 eV, the threshold for absorption of photons by 1s electrons of carbon atoms [23]. The amount of vibrational energy transferred has been estimated to be roughly 20 eV for 288 eV photons [30]. Interestingly, the abundances of the C_2 and Naph+Na fragments are almost equal over the whole energy range (*cf.* Fig. 4), which indicates that they are formed by the same process. Moreover, they are complementary fragments of sodiated rifamycin after loss of acetic acid, which is more intense at high photon energy, like Naph+Na and C_2 (see Fig. 3). This would imply that they come from fragmentation of doubly charged sodiated rifamycin.

Let us now study the influence of double ionization on the photoinduced processes within the sodiated rifamycin dimer. In Fig. 4 (bottom), we plot the relative yield of selected species as a function of photon energy in the 288–300 eV range, where single photoabsorption induces excitation or ejection of one electron of the 1s orbital of a carbon atom, and subsequent Auger electron emission, leading to single or double ionization of the molecular system, respectively. The yield of sodiated rifamycin decreases in this range, but a reverse trend is observed for the C_1 and Naph+Na fragments. Previous works have shown that the relative yield of single ionization of ubiquitin [34] and melittin (two small proteins) after single photoabsorption decreases in the 288–300 eV range, contrary to double ionization: in particular, Bari *et al.* [35] have reported a threshold of 291.4 eV for the latter process in doubly protonated melittin, a value that agrees well with the onset of the rise of C_1 and Naph+Na fragments (see Fig. 4). Therefore, we deduce that intact sodiated rifamycin is mostly created after single ionization and intermolecular fragmentation of the sodiated rifamycin dimer, whereas the C_1 and Naph+Na fragments are formed after double ionization. These results contrast with the enhancement of intermolecular and reduction of intramolecular frag-

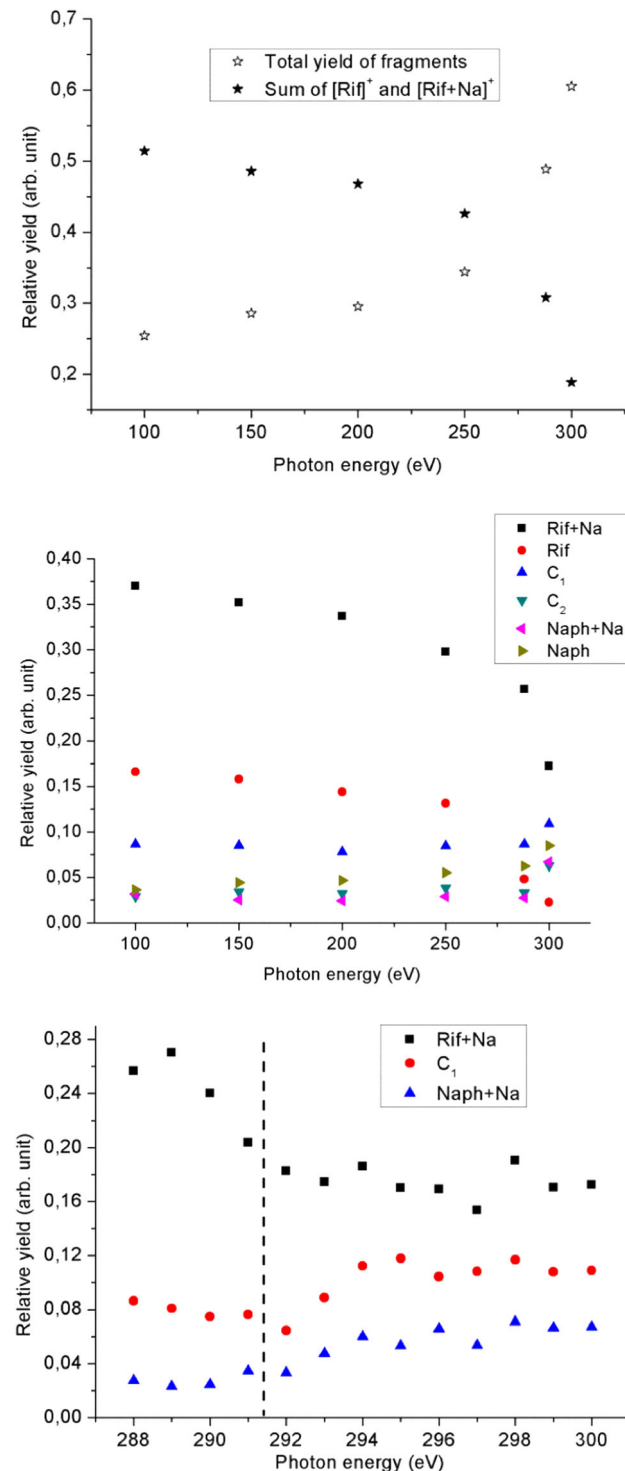


Fig. 4 Total yield of rifamycin fragments (top) and relative yield of selected fragments (middle) together with the yield of monomers formed after photoabsorption of the sodiated rifamycin dimer, as a function of photon energy at 100, 150, 200, 250, 288 and 300 eV (top) and between 288 and 300 eV (bottom, a dashed line appears at 291.4 eV, the threshold reported for double ionization of doubly protonated melittin [35])

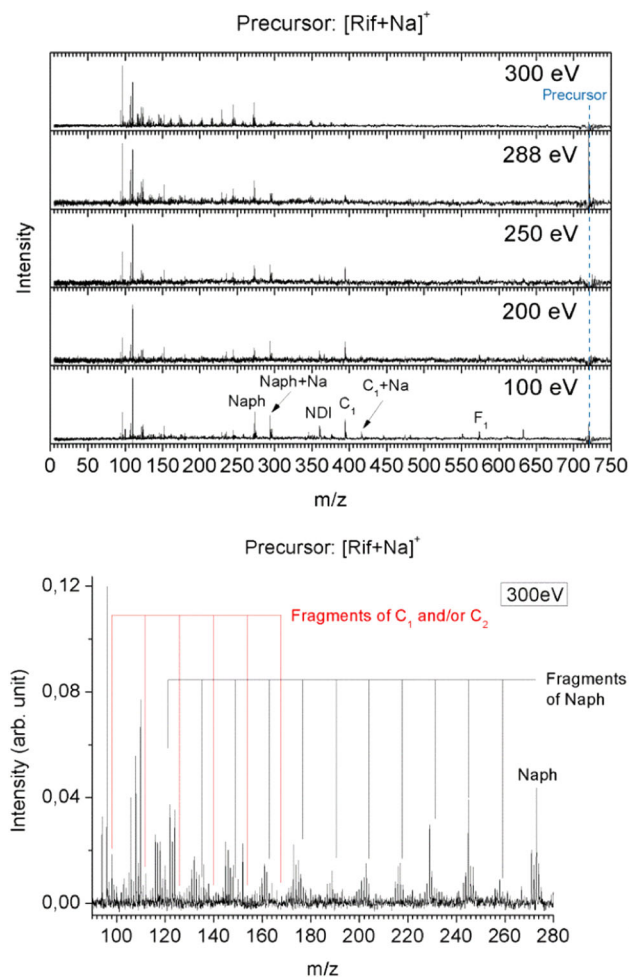


Fig. 5 Top: full mass spectra of sodiated rifamycin after absorption of one soft X-ray photon of different energies. Bottom: zoom into the low-*m/z* range of the 300 eV spectrum

mentation of peptide noncovalent complexes after single photoabsorption that we have reported in this energy range [36]. We attributed this behavior to a transition between electronic excitation and ionization of electrons in 1s orbitals of carbon (leading to single and double ionization, respectively, after Auger electron emission), which would lead to a lower vibrational energy transfer after double ionization. Here, the precursor ion has only one positive charge (against 6 for the peptide complexes); therefore, double ionization allows three fragments to be detected, against only two for single ionization, since only singly charged fragments are seen in the spectra. Thus, some neutral fragments after single ionization become charged after double ionization and can be detected. This might explain the higher yield of these rifamycin fragments.

3.3 X-ray photoabsorption of sodiated rifamycin

Let us now study the photoabsorption of sodiated rifamycin in the same photon energy range as the sodiated dimer (see Sect. 3.2). Figure 5 shows the mass spectra of product cations: they mainly contain peaks already observed in the spectra of the sodiated rifamycin dimer, except the peaks at m/z 360 and m/z 360.5. We attribute them to doubly charged sodiated rifamycin, formed by nondissociative ionization (NDI) of the precursor ion. This assignment is supported by the intensity of the peak at m/z 360.5 being 35% of the one at m/z 360, consistent with the contribution from ^{13}C isotopes of the 37 carbon atoms of sodiated rifamycin. Besides, different groups have previously reported the observation of NDI of several molecular ions of similar size after VUV or X-ray photoabsorption [4, 5, 24, 30, 37]. The NDI peaks decrease in intensity as photon energy rise, while the peaks corresponding to small fragments get more intense, consistent with increasing vibrational energy deposition when photon energy rise. In these mass spectra, we can notice the presence of fragment ions of $m/z < 150$, contrary to the case of the rifamycin dimer. This can be explained by the existence of a threshold in m/z , below which ions are not stored in the Paul trap where precursor ions are irradiated (see Sect. 2). This threshold, but also the maximum m/z that can be stored in the trap, rises with the trap RF amplitude, which has to be higher for the rifamycin dimer. In the region of the 300 eV spectrum containing fragment ions of $m/z < 280$ (see Fig. 5), one can see many groups of peaks separated by m/z 1, indicating sequential fragmentation with extensive H scrambling. We have recently reported such a pattern after X-ray photoabsorption of vancomycin, another antibiotic containing many substituted aromatic rings, and we have attributed this pattern to fragments of these rings. Rifamycin's naphthofuran group consists of two aromatic rings, and starting from the Naph fragment (m/z 273), one can go down in m/z and find a group of peaks roughly every m/z 14, which corresponds to successive losses of the different groups or atoms in rifamycin, *e.g.*, CH_3 , CH_2 , CH , OH , O and NH . The other peaks in this region of the spectrum are assigned to fragments of the C_1 and/or C_2 fragments. The presence of the Naph fragment indicates that sodium can be detached from the naphthofuran group as a result of photoabsorption. It is in line with the peak at m/z 416 that vanishes with increasing photon energy like C_1 does (m/z 394): as for the sodiated rifamycin dimer, it is assigned to C_1+Na . The formation of this fragment ion after photoabsorption in sodiated rifamycin demonstrates that intramolecular sodium transfer occurs. The same process probably explains the presence of the same ion in the spectra of the sodiated rifamycin dimer (see Sect. 3.2). What also supports our assignment of the peak at m/z 416 being due to C_1+Na is the comparison between CID and X-ray spectra: all the most intense peaks in CID spectra are also observed in X-ray spectra and can be assigned to fragments of sodiated or protonated

rifamycin. Moreover, the additional peaks in the X-ray spectra can be attributed to secondary fragmentation of these fragments (*cf.* Fig. 5). The only peaks that cannot be explained this way are m/z 698, 360 and 416. m/z 698 is assigned to proton transfer after ionization, 360 to nondissociative ionization, and 416 to sodium transfer after ionization, which appears consistent. The fact that the latter peak is not observed in our low-energy CID spectra indicates that ionization is required for sodium to be moved from its binding site. Since sodium is bound to a negatively charged group, the photon might be absorbed by the latter, removing one electron and thus the charge, and lowering the binding energy of sodium, leading to its transfer. More work is nevertheless needed to probe this hypothesis and establish if ionization-induced sodium transfer is a widespread process. It would be especially relevant in the context of radiation damage to biological molecular systems, because sodium ions are required in animals for several key functions such as the heart activity, communication between neurons via nerve impulses and electrolyte balance between inside and outside the cell. In the latter process, sodium travels across membrane proteins such as the Na^+/K^- -ATPase enzyme, which binds three sodium ions. The crystal structure of this enzyme revealed the binding sites of sodium, [38] which appear to involve several glutamic and aspartic acid residues. At least some of these are deprotonated and thus carry negative charges located close to the sodium ions, contributing to their binding affinity. Therefore, it seems possible that the removal of electrons from these residues due to ionizing radiation triggers sodium transfer, like in rifamycin. This might prevent the enzyme to function normally, which would be potentially hazardous for the organism.

4 Conclusions

In this report, we show that sodiated rifamycin is a gas-phase molecular salt, by means of CID experiments. Then, we present results from X-ray photoabsorption experiments on sodiated rifamycin dimer and monomer. Absorption of a single photon in the 100–300 eV energy range leads to ionization of the molecular system, followed by vibrational energy deposition and subsequent inter- and/or intramolecular fragmentation. Proton transfer from sodiated rifamycin to rifamycin occurs in the dimer, a widely observed process in ionized molecular systems in the gas phase, consistent with the fact that the dimer is a protonated molecular salt. Contrary to CID at low energy, X-ray photoabsorption triggers sodium transfer in the rifamycin molecular salt. Intramolecular sodium transfer is a process that has not been reported yet, to the best of our knowledge, and is thus worth investigating more deeply. From our results, we cannot know if sodium is transferred as Na^+ or Na , and we do not have access to the fragmentation dynamics, *e.g.* if this transfer occurs before or after fragmentation. Pump-probe experiments at XFEL would thus be

valuable. Moreover, studying this system under absorption of VUV photons from synchrotron radiation would probably allow measuring the photon energy threshold for this process, in the same manner as ionization energies or loss of neutral molecules from protonated peptides for instance [37]. This would give information on the energetics of intramolecular sodium transfer.

Acknowledgements Benoît Colsch is acknowledged for fruitful discussion. This project has received funding from the European Union's Horizon 2020 Research and Innovation Programme under Grant Agreement No. 730872. M. Abdelmouleh is grateful to the PSIME doctoral school (Normandie Université, Caen) for funding a mission in Berlin.

Author contributions

TS designed and built the experimental setup, and JCP wrote the proposal for obtaining the beamtime. The measurements were performed by MA, AER, BB and JCP. AER, JL, PC and JCP did the extensive data analysis of the results. JCP wrote the manuscript, and all authors read it and improved it thanks to their comments.

Data Availability Statement This manuscript has no associated data or the data will not be deposited. [Authors' comment: The data will not be deposited because we could not find a suitable recommended repository for X-ray photoabsorption mass spectra of biomolecular systems.]

References

1. S. Maniam, S. Maniam, *ChemBioChem*. **21**, 3476 (2020)
2. N. Jonker, J. Kool, H. Irth, W.M.A. Niessen, *Anal. Bioanal. Chem.* **399**, 2669 (2011)
3. J. Wang, R. Zhuan, L. Chu, *Sci. Total Environ.* **646**, 1385 (2019)
4. M. Abdelmouleh, M. Lalande, J. El Feghaly, V. Vizcaino, A. Rebelo, S. Eden, T. Schlathölter, J.-C. Pouilly, *J. Am. Soc. Mass Spectrom.* **31**, 1738 (2020)
5. M. Abdelmouleh, M. Lalande, V. Vizcaino, T. Schlatholter, J.-C. Pouilly, *Chem.-a Eur. J.* **26**, 2243 (2020)
6. H.G. Floss, T.W. Yu, *Chem. Rev.* **105**, 621 (2005)
7. E. Sánchez, I. Gutiérrez, M. Luiz, G. Martínez, S. Criado, N.A. García, *Dyes Pigments* **37**, 93 (1998)
8. F. Meier, S. Beck, N. Grassl, M. Lubeck, M.A. Park, O. Raether, M. Mann, *J. Proteome Res.* **14**, 5378 (2015)
9. S. Bari, O. Gonzalez-Magaña, G. Reitsma, J. Werner, S. Schippers, R. Hoekstra, T. Schlathölter, *J. Chem. Phys.* **134**, 024314 (2011)
10. M. Abdelmouleh, M. Lalande, V. Vizcaino, T. Schlathölter, J.-C. Pouilly, *Chem.-A Eur. J.* **26**, 2243 (2020)
11. B. Paizs, S. Suhai, *Mass Spect. Rev.* **24**, 508 (2005)
12. A.M. Alhazmi, P.M. Mayer, *J. Am. Soc. Mass Spect.* **20**, 60 (2009)
13. K. Kumar, B. Siva, N.R. Rao, K.S. Babu, *J. Pharm. Biomed. Anal.* **152**, 224 (2018)
14. K. Chen, N.S. Rannulu, Y. Cai, P. Lane, A.L. Liebl, B.B. Rees, C. Corre, G.L. Challis, R.B. Cole, *J. Am. Soc. Mass Spect.* **19**, 1856 (2008)
15. I. Komaromi, A. Somogyi, V.H. Wysocki, *Int. J. Mass Spect.* **241**, 315 (2005)
16. P. Vouros, D.R. Muller, W.J. Richter, *J. Mass Spect.* **34**, 346 (1999)
17. Y.P. Tu, A.G. Harrison, *J. Mass Spect.* **33**, 858 (1998)
18. M.A.A. Ferreira, C. Borges, M.C. Oliveira, G. Pocsfalvi, A.P. Rauter, A.C. Fernandes, *Int. J. Mass Spect.* **165**, 561 (1997)
19. T.K. Kim, A.K. Hewavitharana, P.N. Shaw, J.A. Fuerst, *Appl. Environ. Microbiol.* **72**, 2118 (2006)
20. S. Kim, J. Chen, T. Cheng, A. Gindulyte, J. He, S. He, Q. Li, B.A. Shoemaker, P.A. Thiessen, B. Yu, L. Zaslavsky, J. Zhang, E.E. Bolton, *Nucl. Acids Res.* **47**, D1102 (2019)
21. N.P. Lopes, P.J. Gates, J.P.G. Wilkins, J. Staunton, *Analyst* **127**, 1224 (2002)
22. B. Colsch, A. Damont, C. Junot, F. Fenaille, J.-C. Tabet, *Eur. J. Mass Spectrom.* **25**, 333 (2019)
23. A.R. Milosavljevic, F. Canon, C. Nicolas, C. Miron, L. Nahon, A. Giuliani, *J. Phys. Chem. Lett.* **3**, 1191 (2012)
24. L. Schwob, M. Lalande, J. Rangama, D. Egorov, R. Hoekstra, R. Pandey, S. Eden, T. Schlatholter, V. Vizcaino, J.-C. Pouilly, *Phys. Chem. Chem. Phys.* **19**, 18321 (2017)
25. J.-C. Pouilly, V. Vizcaino, L. Schwob, R. Delaunay, J. Kocisek, S. Eden, J.-Y. Chesnel, A. Mery, J. Rangama, L. Adoui, B. Huber, *Chemphyschem* **17**, 325 (2016)
26. C.-C. Shen, T.-T. Tsai, J.-Y. Wu, J.-W. Ho, Y.-W. Chen, P.-Y. Cheng, *J. Chem. Phys.* **147**, 164302 (2017)
27. C. Leidlmair, P. Bartl, H. Schobel, S. Deniff, S.F. Yang, A.M. Ellis, P. Scheier, *Chemphyschem* **13**, 469 (2012)
28. A. Golan, K.B. Bravaya, R. Kudirka, O. Kostko, S.R. Leone, A.I. Krylov, M. Ahmed, *Nat. Chem.* **4**, 323 (2012)
29. K. Ohta, Y. Matsuda, N. Mikami, A. Fujii, *J. Chem. Phys.* **131** (2009)
30. D. Egorov, L. Schwob, M. Lalande, R. Hoekstra, T. Schlatholter, *Phys. Chem. Chem. Phys.* **18**, 26213 (2016)
31. X. Liang, J. Liu, Y. Leblanc, T. Covey, A.C. Ptak, J.T. Brenna, S.A. McLuckey, *J. Am. Soc. Mass Spectrom.* **18**, 1783 (2007)
32. V. Blagojevic, D.K. Bohme, *Chempluschem* **78**, 1049 (2013)
33. S. Hoyau, K. Norrman, T.B. McMahon, G. Ohanessian, *J. Am. Chem. Soc.* **121**, 8864 (1999)
34. A.R. Milosavljevic, C. Nicolas, M.L.J. Rankovic, F. Canon, C. Miron, A. Giuliani, *J. Phys. Chem. Lett.* **6**, 3132 (2015)
35. S. Bari, D. Egorov, T.L.C. Jansen, R. Boll, R. Hoekstra, S. Techert, V. Zamudio-Bayer, C. Buelow, R. Lindblad, G. Leistner, A. Lawicki, K. Hirsch, P.S. Miedema, B. von Issendorff, J.T. Lau, T. Schlatholter, *Chem.-a Eur. J.* **24**, 7631 (2018)

36. M. Lalande, M. Abdelmouleh, M. Ryszka, V. Vizcaino, J. Rangama, A. Mery, F. Durante, T. Schlatholter, J.-C. Poully, *Phys. Rev. A* **98**, 062701 (2018)
37. F. Canon, A.R. Milosavljevic, L. Nahon, A. Giuliani, *Phys. Chem. Chem. Phys.* **17**, 25725 (2015)
38. R. Kanai, H. Ogawa, B. Vilsen, F. Cornelius, C. Toyoshima, *Nature* **502**, 201 (2013)